



Hydrogen isotope fractionation during lipid biosynthesis by *Haloarcula marismortui*

Sitindra S. Dirghangi*, Mark Pagani

Department of Geology and Geophysics, Yale University, New Haven, CT 06511, USA

Received 20 November 2012; accepted in revised form 17 May 2013; Available online 30 May 2013

Abstract

We studied the controls on the fractionation of hydrogen isotopes during lipid biosynthesis by *Haloarcula marismortui*, a halophilic archaea, in pure culture experiments by varying organic substrate, the hydrogen isotope composition (D/H) of water, temperature, and salinity. Cultures were grown on three substrates: succinate, pyruvate and glycerol with known hydrogen isotope compositions, and in water with different hydrogen isotopic compositions.

All culture series grown on a particular substrate show strong correlations between $\delta D_{\text{archaeol}}$ and δD_{water} . However, correlations are distinctly different for cultures grown on different substrates. Our results indicate that the metabolic pathway of substrate exerts a fundamental influence on the δD value of lipids, likely by influencing the D/H composition of NADPH (nicotinamide adenine dinucleotide phosphate), the reducing agent that contributes hydrogen to carbon atoms during lipid biosynthesis. Temperature and salinity have smaller, but similar effects on δD_{lipid} , primarily due to the way temperature and salinity influence growth rate, as well as temperature effects on the activity of enzymes.

© 2013 Elsevier Ltd. All rights reserved.

1. INTRODUCTION

An important aspect of paleoclimate research is the determination of hydrological conditions during periods of rapid global change or distinctively different climate states. Changes in hydrological conditions can be expressed by changes in the hydrogen isotopic composition of precipitation (D/H_{precip}) given that D/H_{precip} is determined by the source-water D/H (Dansgaard, 1964; Craig and Gordon, 1965; Gat, 1996), the distance and route of vapor transport (Yamanaka et al., 2004), humidity at the source of evaporation (Craig and Gordon, 1965; Merlivat and Jouzel, 1979), and the temperature at the site of evaporation and precipitation (Dansgaard, 1964; Jouzel et al., 1987). There are several ways to approach the reconstruction of hydrologic signals in the geologic record (Savin and Epstein, 1970; Peete et al., 1990; Stern et al., 1997; Barker et al., 2001; Shuman et al., 2002). Recently, proxy records of D/H_{precip} have

been reconstructed from the hydrogen isotopic compositions of lipids (D/H_{lipid}) of algae (Huang et al., 1995; Sauer et al., 2001) and higher-plant waxes (Xie et al., 2000; Huang et al., 2002; Yang and Huang, 2003; Sachse et al., 2004, 2009; Schefuß et al., 2005; Hou et al., 2006; Shuman et al., 2006; Smith and Freeman, 2006).

D/H_{lipid} of plants and other photoautotrophic organisms is dependent on the hydrogen isotope composition of source water used during photosynthesis, but lipids are significantly D-depleted compared to water, due to biosynthetic effects. However, environmental conditions of growth that impact growth rate of the organism, enzyme activity, and rate of metabolism can also alter isotope fractionations during lipid synthesis. For example, cultures of marine haptophyte algae, *Emiliania huxleyi* and *Gephyrocapsa oceanica*, show that alkenone δD values decrease with higher growth rates, and increase with higher salinity (Schouten et al., 2006). Alkenones in *E. huxleyi* became D-depleted with temperature increase from 10 °C to 15 °C but became D-enriched with further temperature increase from 15 °C to 21 °C (Schouten et al., 2006), possibly because of 15 °C being the optimal growth temperature

* Corresponding author.

E-mail address: sitindra.dirghangi@yale.edu (S.S. Dirghangi).

(Zhang et al., 2009b), and in *G. oceanica*, alkenones became D-depleted with temperature increase from 15 °C to 21 °C (Schouten et al., 2006). A decrease in δD_{lipid} with increasing temperature was also observed for two strains of freshwater algae, *Eudorina unicocca* and *Volvox aureus* (Zhang et al., 2009b). Further, isoprenoid lipids (sterols) of marine diatom *Thalassiosira pseudonana* were substantially more D-enriched when grown in nitrate-limited cultures, whereas D/H ratios of fatty acids were similar under nitrate-limited and nitrate-replete conditions (Zhang et al., 2009b).

In addition to source-water hydrogen and environmental conditions, distinct hydrogen isotope fractionations are associated with the biosynthesis of fatty acids and isoprenoids, including the mevalonate (MVA) and non-mevalonate (non-MVA) pathways (Sessions et al., 1999, 2002; Zhang and Sachs, 2007; Zhang et al., 2009a,b). Differences in carbon chain-length and the degree of saturation are also known to contribute to hydrogen isotope signatures (Chikaraishi et al., 2004; Zhang and Sachs, 2007). Further, the same lipid synthesized by different families of freshwater algae exhibit significantly different hydrogen isotope compositions (Zhang and Sachs, 2007). This variability cannot be explained by changes in source water, environmental conditions or biosynthetic pathways (Zhang and Sachs, 2007), and point to the isotopic influence and proportion of hydrogen derived from the reducing agent nicotinamide adenine dinucleotide phosphate (NADPH), as well as the potential for different pools of NADPH with distinct isotopic signatures (Zhang et al., 2009a). Importantly, NADPH and acetate contribute the majority of all carbon-bound hydrogen in lipids. While the δD value of acetate is determined by the metabolism of the available organic substrate, NADPH is generated by various reactions in various metabolic pathways, including glycolysis, pentose phosphate pathway, and the tricarboxylic acid (TCA) cycle (Csonka and Fraenkel, 1977), with widely different D/H fractionations associated with each (Zhang et al., 2009a).

Compared to photoautotrophs, few studies have focused on the hydrogen isotopic composition of lipids from heterotrophic prokaryotes, and in particular the isotopic nature of archaeal lipids. Zhang et al. (2009a) observed a wide range of $\epsilon_{\text{lipid-water}}$ in four strains of heterotrophic bacteria: *Cupriavidus oxalaticus*, *Cupriavidus necator*, *Escherichia coli* and *Rhodospseudomonas palustris*, cultured on various organic substrates. They reviewed evidence suggesting that NADPH is the most important factor controlling the magnitude of $\epsilon_{\text{lipid-water}}$ and contributes ~50% of all carbon-bound hydrogen, while water and hydrogen associated with the substrate each contribute ~25%.

Kaneko et al. (2011) analyzed D/H compositions of isoprenoid biphytane chains from glycerol dialkyl glycerol tetraethers (GDGTs) by ether-bond cleavage with HI followed by hydrogenation with H_2/PtO_2 . Their results demonstrate that isoprenoid biphytane chains from GDGTs synthesized by *Sulfolobus shibatae* are D-depleted compared to the growth water. The magnitude of D-depletion was larger than algal fatty acids, but less than phytol, whereas biphytanes from marine sedimentary GDGTs had similar D/H range as eukaryal and bacterial isoprenoids. Isotopic differences between biphytanes from *Sulfolobus* cultures and

marine sediments potentially arise from thermophilic growth in freshwater for *Sulfolobus* and mesophilic growth in seawater for marine crenarchaea (Kaneko et al., 2011). D-enrichment was also observed with formation of cyclopentane rings (Kaneko et al., 2011). However, the D/H fractionation during lipid biosynthesis by archaea is yet to be thoroughly studied and understood.

For this study, we cultured the halophilic euryarchaea *Haloarcula marismortui* to assess hydrogen isotope fractionations associated with the biosynthesis of archaeol (an isoprenoidal diether lipid). *H. marismortui* is heterotrophic, providing the opportunity to study effects of organic substrate on D/H_{lipid} , as well as temperature and salinity.

Archaeol is a common lipid observed in both euryarchaea and crenarchaea (Boucher, 2007), but, in hypersaline environments, halophilic archaea are the dominant source of archaeol. Stiehl et al. (2005) found archaeol in three strains of halophilic archaea, including *H. marismortui* which was initially isolated from the Dead Sea by Oren et al. (1990) and subsequently grown in pure cultures. Diether lipids were the dominant lipids observed in these cultures, and indeed, halophilic archaea were reported to be the only source of archaeol in Dead Sea sediments (Stiehl et al., 2005). Our findings, therefore, may also be of interest in paleoclimatological research.

2. MATERIALS AND METHODS

2.1. Culture experiments

We performed pure culture experiments to test the impact of carbon source, temperature, and salinity on the hydrogen isotopic fractionation associated with lipid biosynthesis in *H. marismortui*. The *H. marismortui* strain was provided by P.B. Moore at Yale University. *H. marismortui* was grown in 200 ml batch cultures in 1 L Erlenmeyer flasks, in a growth media consisting of 184 g/L NaCl, 23 g/L $MgCl_2 \cdot 6H_2O$, 26.845 g/L $MgSO_4 \cdot 7H_2O$, 5.369 g/L KCl, 0.5635 g/L $CaCl_2$, 5 l/L 1 M NH_4Cl , and trace amounts of K_2HPO_4 , $MnCl_2 \cdot 4H_2O$, $ZnSO_4 \cdot 7H_2O$, $FeSO_4 \cdot 7H_2O$, $CuSO_4 \cdot 5H_2O$, thiamine and biotin (Dyall-Smith, 2009). Three different organic substrates for growth were used: Na-Succinate hexahydrate (8.3 g/L), Na-Pyruvate (5 g/L), and Glycerol (5 ml/L). For all experiments where organic substrate was varied, the pH of the media was maintained at 7.5. The cultures were grown in incubators and shaker baths for controlling temperature. Light availability was not systematically controlled and the cultures were shaken once in an hour throughout the incubation period. The flasks were not sealed and were covered with aluminium foils. Cultures were grown for 4 days at 45 °C, and extracted during the stationary phase.

For salinity experiments, cultures were grown at 45 °C under three salt concentrations: 23%, 25% and 30%. Compositions of these culture media are presented in Table 1. Cultures for temperature experiments were grown in 23% salinity at 32, 40 and 45 °C. The compositions of the media used for temperature experiments are also shown in Table 1. All cultures were grown for 4 days and extracted during the stationary phase.

Table 1
Composition of media and growth conditions for the cultures grown at different temperatures and salinities.

Sample name	δD_{water} (‰)	Salinity (%)	Temperature (°C)	NaCl (g/L)	MgCl ₂ ·6H ₂ O (g/L)	MgSO ₄ ·7H ₂ O (g/L)	KCl (g/L)	CaCl ₂ (g/L)	Oxoid Peptone (g/L)	Yeast Extract (g/L)
<i>Temperature experiments</i>										
HMa_Ia	−55	23	32	184	23	26.85	5.37	0.56	5	1
HMa_Ib	32	23	32	184	23	26.85	5.37	0.56	5	1
HMa_IIa	−55	23	40	184	23	26.85	5.37	0.56	5	1
HMa_IIb	32	23	40	184	23	26.85	5.37	0.56	5	1
HMa_IIIa	−55	23	45	184	23	26.85	5.37	0.56	5	1
HMa_IIIb	32	23	45	184	23	26.85	5.37	0.56	5	1
<i>Salinity experiments</i>										
HMa_IIIa	−55	23	45	184	23	26.85	5.37	0.56	5	1
HMa_IIIb	32	23	45	184	23	26.85	5.37	0.56	5	1
HMa_IVa	−55	25	45	200	25	29.18	5.84	0.61	5	1
HMa_IVb	32	25	45	200	25	29.18	5.84	0.61	5	1
HMa_Va	−55	30	45	240	30	35.00	7.00	0.74	5	1
HMa_Vb	32	30	45	240	30	35.00	7.00	0.74	5	1

Deuterium-enriched growth media was produced by adding aliquots of 99%-pure D₂O to the media. After preparation, all media were sterilized by autoclaving prior to inoculation. A 5–6 ml starter culture was grown in unlabeled media for 3 days (early stationary phase) and 100 μ l aliquots of the starter culture were used to inoculate all the cultures. The starter culture and all the cultures were checked for purity by microscopy.

Growth curves were obtained with a spectrophotometer (DU 640, Beckman Instruments Inc.) by measuring optical density (i.e. absorbance) at 600 nm (Fig. S1). Growth rate (Divisions day^{−1}) was calculated as follows (Zhang et al., 2009b):

$$k = \log_2(N_1/N_0)/(T_1 - T_0) \quad (1)$$

where k is growth rate, N_0 and N_1 denote respectively the optical density at the beginning and the end of the exponential growth phase, T_0 and T_1 denote respectively the time at the beginning and the end of the exponential growth phase.

2.2. Lipid extraction and analysis

For lipid extraction, cultures were centrifuged and freeze-dried. Lipids were extracted by sonication using 1:1(v/v) dichloromethane:methanol followed by 2:1(v/v) dichloromethane:methanol. Basic hydrolysis was performed on total lipid extracts (TLE) by adding \sim 5 ml of 2 N potassium hydroxide dissolved in a 9:1(v/v) mixture of water:methanol to TLEs and keeping the mixture at 80 °C for 2 h, subsequently cooled, and 5% sodium chloride aqueous solution (5 ml) was added. The neutral lipid fraction was then extracted with dichloromethane and separated into three fractions by silica–gel chromatography with 2 ml of hexane, followed by 4 ml of dichloromethane, and finally 4 ml of methanol. Methanol fractions were concentrated under a stream of nitrogen, dissolved in hexane, and examined for archaeol using a ThermoFinnigan Trace GC-FID fitted with a Restek Rxi[®]-1 ms column (60 m,

0.25 mm ID, 0.25 μ m df). Methanol fractions were not derivatized prior to analysis. The injector (programmable temperature vaporizer or PTV) temperature program was 80 °C for 0.30 min, and heating to 320 °C at a rate of 14.5 °C/s. The oven temperature program was 60 °C for 1 min, increasing to 320 °C at a rate of 7 °C/min, and maintaining 320 °C for 30 min. Archaeol (underivatized) eluted at \sim 39 min (Fig. S2).

2.3. Hydrogen isotope analysis of water, substrates and lipids

Hydrogen isotope compositions of the growth media were measured at the beginning of the culture experiments on aliquots (\sim 4 ml) collected prior to inoculation in duplicate using a Thermo Finnigan MAT 253 isotope ratio monitoring mass spectrometer coupled to a Thermo H-Device. The δD_{water} values were corrected using in-house water standards normalized to VSMOW-SLAP scale and are expressed relative to VSMOW. Analytical precision for δD_{water} measurements was $\pm 3\text{‰}$. In order to decipher δD values of the non-exchangeable hydrogen in the substrates, they were equilibrated with two different waters with different δD following the protocol described by Qi and Coplen (2011). Following the equilibration experiments, substrates were analyzed using a Thermo Delta Plus XP coupled to a TC/EA. δD values of the non-exchangeable C-bound hydrogen of pyruvate, succinate and glycerol were -97‰ , -382‰ and -61‰ , respectively. δD values of Oxoid Peptone and Yeast Extract used in temperature and salinity experiments were -65‰ and -95‰ , respectively. However, a significant amount of uncertainty may be associated with these calculations (up to $\pm 20\text{‰}$; Zhang et al., 2009a). δD values of lipids were measured by isotope ratio monitoring Gas Chromatography–Mass Spectrometry using a Finnigan MAT 253 stable isotope mass spectrometer coupled to a Thermo Trace2000 GC with a high temperature conversion system. The H_3^+ factor for the GC-IRMS was measured daily prior to δD analysis, with a mean value for the measurement periods of 16.12 ± 0.39 (1 σ). We used n -al-

kane isotope standards (Mix A, Indiana University Biogeochemical Laboratory) and an in-house standard consisting of three long chain *n*-alkanes: octatriacontane (C₃₈), hentacontane (C₄₁), *n*-tetratriacontane (C₄₄), to monitor instrument accuracy and stability. The in-house mixture was run separately with the samples. Elution times for C₄₁ and C₄₄ bracketed the archaeol peak. Archaeol δD values were corrected using known isotopic values of C₄₁ and C₄₄. Analytical precision of isotopic analyses for the C₄₁ and C₄₄ alkane standards were $\pm 3.1\%$ and $\pm 2.9\%$, respectively. All lipid samples were measured in duplicate. Hydrogen isotope data were calculated as follows:

$$\delta D = R_{\text{sample}}/R_{\text{std}} - 1 \quad (2)$$

where $R_{\text{sample}} = (D/H)_{\text{sample}}$, $R_{\text{std}} = (D/H)_{\text{VSMOW}}$, VSMOW represents Vienna Standard Mean Ocean Water.

$$\alpha_{A-B} = (\delta D_A + 1)/(\delta D_B + 1) \quad (3)$$

$$\varepsilon_{A-B} = \alpha_{A-B} - 1 \quad (4)$$

where A and B represent lipids (archaeol) and water or substrate, respectively.

3. RESULTS

3.1. Growth rates of *H. marismortui*

Growth rates of *H. marismortui* did not show significant variations when grown on different substrates (Fig. S1). Growth rates were 1.32, 1.26 and 1.24 divisions day⁻¹ for cultures grown on pyruvate, succinate and glycerol, respectively. Growth rates were different for cultures grown at different temperatures and salinities (Fig. S1). For cultures grown at 32 °C, 40 °C and 45 °C, growth rates were respectively 1.87, 2.81 and 2.7 divisions day⁻¹. Cultures grown at 23%, 25% and 30% salinities showed growth rates of 2.7, 2.95 and 1.54 divisions day⁻¹, respectively.

3.2. Hydrogen isotopic composition of lipids

Archaeol was abundant in all cultures of *H. marismortui*. This agrees with previous culture experiments with halophilic archaea, where archaeol was found to be a major lipid constituent of halophilic archaea (Stiehl et al., 2005). In all cultures, archaeol was substantially D-depleted relative to environmental water and varied depending on the carbon source used for growth (Table 2). For cultures grown on pyruvate (δD : -97%), with δD_{water} values ranging from -29% to 183% , $\delta D_{\text{archaeol}}$ ranged from -131% to 32% . In cultures grown on succinate (δD : -382%), $\delta D_{\text{archaeol}}$ ranged from -89% to 37% and on glycerol (δD : -61%), $\delta D_{\text{archaeol}}$ ranged from -227% to -113% . In all cultures, strong correlations are observed between the D/H composition of archaeol and growth water ($R^2 = 0.97$ to 0.99), although slopes and intercepts of correlations were different depending on the organic substrate used for metabolism (Table 2, Fig. 1).

We calculated ε values (Eq. (3)) between archaeol, water, and substrates in order to estimate the D/H fractionation between archaeol–water and archaeol–substrate (Table 2). Average $\varepsilon_{\text{archaeol-water}}$ values were -122% for *H.*

marismortui grown on pyruvate, -103% for cultures grown on succinate and -228% for cultures grown on glycerol.

Distinct temperature effects on the magnitude of $\varepsilon_{\text{archaeol-water}}$ were also observed, with archaeol D-depleted compared to growth water for all temperature experiments. For δD_{water} values of -55% and 32% , $\delta D_{\text{archaeol}}$ values were: -177% and -128% at 32 °C, -191% and -150% at 40 °C, and -181% and -141% at 45 °C (Table 3, Fig. 2a).

Archaeol was D-depleted compared to the D/H of water in all the cultures grown at different salinities. For δD_{water} values -55% and 32% , $\delta D_{\text{archaeol}}$ values were: -181% and -141% at 23% salinity, -191% and -168% at 25% salinity, and -189% and -152% at 30% salinity (Table 3, Fig. 2b).

4. DISCUSSION

4.1. Cultures grown on different substrates

Lipid hydrogen of heterotrophic archaea can derive from water, the organic substrate, and reducing agents such as NADPH (Sessions et al., 2002; Zhang et al., 2009a). Our experiments show that the D/H composition of archaeol correlate well with δD_{water} in all cultures, indicative of a first-order control by water on lipid δD (δD_{lipid}) values (Fig. 1). Our results also show that δD_{lipid} values are also substantially influenced by the type of carbon source used during growth. However, a simple substrate D/H inheritance cannot explain our results. Archaeol is consistently D-enriched relative to succinate, but D-depleted relative to glycerol and range from slightly D-depleted to D-enriched (depending on the δD_{water}) relative to pyruvate (Table 2), in contrast to the relative hydrogen isotope compositions of the substrates (Table 2, Fig. 1). Interestingly, archaeol is always D-depleted relative to water, irrespective of the substrate used, and the value of $\varepsilon_{\text{archaeol-water}}$ with glycerol ($\varepsilon = -228\%$) was greater than $\varepsilon_{\text{archaeol-water}}$ using pyruvate ($\varepsilon = -122\%$) or succinate ($\varepsilon = -103\%$). Ultimately, these results point to substantial D/H fractionation associated with the metabolism of substrates that result in the formation of the acetyl CoA precursor, and most importantly, to processes that affect the hydrogen isotopic composition of NADPH. Indeed, other cultures of heterotrophic bacteria have indicated that differences in the hydrogen isotope composition of NADPH associated with the metabolism of different organic substrates is potentially the most important factor controlling D/H ratios of their lipids (Zhang et al., 2009a).

Comparison of our results (Table 2) with other heterotrophic bacterial cultures (Table 4) shows both consistent and contrasting fractionation patterns. For example, *C. necator* grown on pyruvate produced fatty acids D-enriched relative to source water, whereas *E. coli* produced fatty acids D-depleted relative to water when grown on pyruvate (Zhang et al., 2009a). In contrast, for this study, *H. marismortui* grown on pyruvate produced archaeol that was D-depleted relative to water. Metabolism of pyruvate by *H. marismortui* involves decarboxylation to acetyl CoA, and then a major portion of acetyl CoA ($\sim 90\%$) enters the

Table 2
Hydrogen isotope data from cultures grown on different substrates.

Name	Substrate	$\delta D_{\text{substrate}} (\text{‰})$	$\delta D_{\text{water}} (\text{‰})$	$\delta D_{\text{archaeol}} (\text{‰})$	St. dev. (σ)	$\epsilon_{\text{archaeol-substrate}} (\text{‰})$	$\epsilon_{\text{archaeol-water}} (\text{‰})$
HMa_py_I	Pyruvate	-97	-29	-131	0.6	-38	-105
HMa_py_II	Pyruvate	-97	69	-69	0.5	31	-129
HMa_py_III	Pyruvate	-97	126	-15	2	91	-125
HMa_py_IV	Pyruvate	-97	183	32	1.8	143	-128
HMa_suc_I	Succinate	-382	-30	-89	0.1	473	-61
HMa_suc_II	Succinate	-382	69	-49	0.6	537	-111
HMa_suc_III	Succinate	-382	125	-8	2.4	604	-118
HMa_suc_IV	Succinate	-382	179	37	1.7	678	-120
HMa_gl_I	Glycerol	-61	-29	-227	1.9	-177	-204
HMa_gl_II	Glycerol	-61	69	-175	0.3	-122	-228
HMa_gl_III	Glycerol	-61	126	-133	0.5	-77	-229
HMa_gl_IV	Glycerol	-61	183	-113	2.4	-56	-251

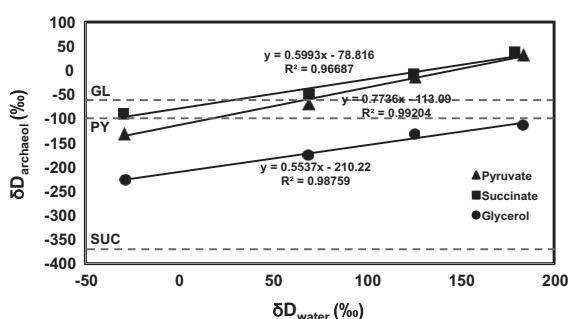


Fig. 1. Data from the culture experiments on different substrates, $\delta D_{\text{archaeol}}$ plotted against the δD_{water} . δD values of glycerol (GL), pyruvate (PY), and succinate (SUC) are represented by three dashed lines.

TCA cycle (Falb et al., 2008). When grown on succinate, both *C. necator* and *C. oxalaticus* fatty acids were D-enriched compared to water (Zhang et al., 2009a), while our cultures of *H. marismortui* produced archaeol that was D-depleted relative to water. Succinate is an intermediate compound in the TCA cycle (Fig. S3). Finally, when carbohydrates were used as substrates for bacteria (Zhang et al., 2009a), and glycerol was used as substrate for *H. marismortui*, lipids from all cultures were D-depleted relative to water. Glycerol metabolism by *H. marismortui* involves conversion to pyruvate that subsequently participates in

the TCA cycle (Fig. S3). (Note: we assume results for carbohydrates and glycerol are comparable as glycerol metabolism partly follows the glycolytic pathway (Fig. S3), which is also followed during carbohydrate metabolism).

Processes that affect the D/H ratios of NADPH are crucial in controlling the hydrogen isotope ratios of lipids, as previous culture experiments demonstrate that NADPH is the dominant source of hydrogen in lipids (Zhang et al., 2009a). During reduction of NADPH, H^+ is transferred directly from the reactant molecule to $NADP^+$ (Zhang et al., 2009a), which is associated with a large, normal isotopic fractionation (Zhang et al., 2009a). In spite of that, we observe D-enrichment of lipids compared to the organic substrate and in some cases compared to the growth water (Zhang et al., 2009a). Zhang et al. (2009a) proposed two mechanisms that could account for the observed isotopic enrichment. The first mechanism involves two reactions in the TCA cycle accompanied by NADPH reduction which include (i) conversion of isocitrate to α -ketoglutarate (or 2-oxoglutarate) and (ii) malate to pyruvate, catalyzed by isocitrate dehydrogenase and malic enzyme, respectively (Fig. S3), during which H in NADPH is obtained from an OH-C-H group in the reactant molecule, which contains only one H. These OH-C-H groups are D-enriched and H^+ transfer from these OH-C-H groups to $NADP^+$ can potentially result in D-enriched NADPH (Zhang et al., 2009a and references therein). This proposed mechanism for heterotrophic bacteria is also relevant for halophilic archaea because all the enzymes involved in

Table 3
Hydrogen isotope data from cultures grown at different temperatures and salinities.

Sample name	T ($^{\circ}C$)	Salinity (%)	NaCl (mol/L)	$\delta D_{\text{archaeol}} (\text{‰})$	St. dev. (σ)	$\delta D_{\text{water}} (\text{‰})$	$\epsilon_{\text{archaeol-water}} (\text{‰})$
HMa_Ia	32	23	3.15	-177	3	-55	-126
HMa_Ib	32	23	3.15	-128	0.8	32	-156
HMa_IIa	40	23	3.15	-191	0.8	-55	-143
HMa_IIb	40	23	3.15	-150	3.3	32	-176
HMa_IIIa	45	23	3.15	-181	0.5	-55	-133
HMa_IIIb	45	23	3.15	-141	0.6	32	-167
HMa_IVa	45	25	3.42	-191	2.2	-55	-143
HMa_IVb	45	25	3.42	-168	0.6	32	-193
HMa_Va	45	30	4.1	-189	8.9	-55	-141
HMa_Vb	45	30	4.1	-152	1.3	32	-178

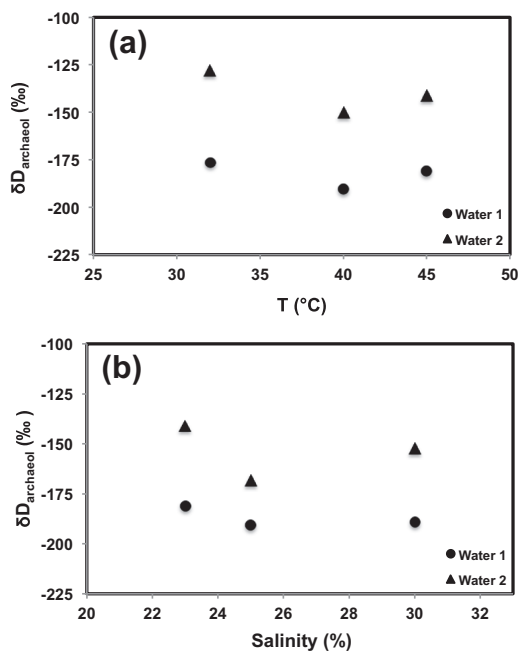


Fig. 2. Data from the cultures grown at different temperatures and salt concentrations. (a) $\delta D_{\text{archaeol}}$ plotted against temperature. (b) $\delta D_{\text{archaeol}}$ plotted against salinity. Water 1 and 2 represent growth waters with δD values of -55‰ and 32‰ , respectively.

NADPH-reducing reactions are observed in halophilic archaea (Falb, 2005). A second mechanism that could lead to lipid D-enrichment involves the conversion of NADPH to NADH catalyzed by the enzyme transhydrogenase, which is a mechanism for controlling the amount of NADPH (Zhang et al., 2009a and references therein). This process also involves significant isotope fractionation and can make δD_{NADPH} significantly D-enriched (Zhang et al., 2009a). However, this mechanism seems unlikely to explain our observations, as known transhydrogenase enzymes are not found in *H. marismortui* (Anderson et al., 2011).

Glycerol metabolism, on the other hand, follows the glycolytic pathway that involves only one NADPH reducing reaction (Fig. S3) – the conversion of glyceraldehyde-3-phosphate to 1,3-bisphosphoglycerate catalyzed by glyceraldehydes-3-phosphate dehydrogenase. H^+ is transferred in this reaction from a terminal CHO group in the reactant molecule to $NADP^+$. Unlike the TCA cycle reactions mentioned previously (Zhang et al., 2009a), this CHO group does not undergo D-enrichment in the previous steps of the pathway (Fig. S3). Therefore, the resulting NADPH from this reaction should be D-depleted, possibly resulting in the lipids synthesized by *H. marismortui* grown on glycerol being more D-depleted than ambient water.

Growth on pyruvate yields different fractionations in this study and in two heterotrophic bacteria investigated by Zhang et al. (2009a). *C. necator* fatty acids are up to 97‰ D-enriched, *E. coli* fatty acids are up to -60‰ D-depleted (Zhang et al., 2009a; Table 4) and archaeol in the current study is -122‰ D-depleted compared to growth water. It is surprising that pyruvate metabolism in three

Table 4
Hydrogen isotope data from three strains of heterotrophic bacteria studied by Zhang et al. (2009a).

Organism	Cultures	Substrate	$\delta D_{\text{substrate}}$ (‰)	δD_{water} (‰)	$\delta D_{16:0}$ (‰)	$\epsilon_{16:0\text{-water}}$ (‰)	$\epsilon_{16:0\text{-substrate}}$ (‰)	$\delta D_{16:1}$ (‰)	$\epsilon_{16:1\text{-water}}$ (‰)	$\epsilon_{16:1\text{-substrate}}$ (‰)	$\delta D_{18:1}$ (‰)	$\epsilon_{18:1\text{-water}}$ (‰)	$\epsilon_{18:1\text{-substrate}}$ (‰)
<i>C. necator</i>	Cn2-I	Fructose	-22	-65.5	-101	-38	-81	-137	-77	-118	-110	-48	-90
<i>C. necator</i>	Cn4-I	Pyruvate	-12	-64.4	26	97	38	-12	56	0.00	8	77	20
<i>C. necator</i>	Cn6-I	Succ-1 (succinate)	-97	-68.6	89	169	206	51	128	164	62	140	176
<i>C. necator</i>	Cn7-I	Succ-2 (succinate)	-97	-68.6	-3	70	104	-35	36	69	-34	37	70
<i>E. coli</i>	Ec1-I	Glucose	-60	-61.9	-178	-124	-126	-176	-122	-123	-173	-118	-120
<i>E. coli</i>	Ec3-I	Pyruvate	-12	-68.1	-120	-56	-109	-124	-60	-113	-108	-43	-97
<i>E. coli</i>	Ec5-I	Glucose	-60	-60	-180	-128	-128	-197	-146	-146	-183	-131	-131
<i>E. coli</i>	Ec5-II	Glucose	-60	49.9	-128	-169	-72	-122	-164	-66	-122	-164	-66
<i>E. coli</i>	Ec5-III	Glucose	-60	152	-44	-170	17	-68	-191	-9	-44	-170	17
<i>E. coli</i>	Ec5-IV	Glucose	-60	314	57	-196	124	30	-216	96	50	-201	117
<i>C. oxalaticus</i>	Co5-I	Succinate	-97	-64.3	109	185	228	64	137	178	77	151	193
<i>C. oxalaticus</i>	Co5-II	Succinate	-97	41.1	219	171	350	176	130	302	205	157	334
<i>C. oxalaticus</i>	Co5-III	Succinate	-97	121.1	282	144	420	235	102	368	266	129	402
<i>C. oxalaticus</i>	Co5-IV	Succinate	-97	214.1	331	96	474	296	67	435	326	92	468
<i>C. oxalaticus</i>	Co6-II	Succinate	-97	41.1	166	120	291	106	62	225	128	83	249
<i>C. oxalaticus</i>	Co6-III	Succinate	-97	121.1	226	94	358	163	37	288	184	56	311
<i>C. oxalaticus</i>	Co6-IV	Succinate	-97	214.1	302	72	442	238	20	371	258	36	393

heterotrophic organisms would lead to formation of significantly different δD_{NADPH} and δD_{lipid} values. One possible explanation could be that the portion of pyruvate (or acetyl CoA generated from pyruvate) utilized for various biochemical pathways (e.g. TCA cycle, gluconeogenesis, and synthesis of lipid, formate, lactate, alanine) vary for different organisms. As a result, the δD of the pool of pyruvate (or acetyl CoA) utilized for lipid synthesis could be different, as reflected by variations in δD_{lipid} . Alternatively, even though these organisms are grown on the same organic substrate (pyruvate), the rates of different reactions affecting hydrogen isotopic composition of NADPH are different, leading to distinctly different δD_{NADPH} , and consequently, different δD_{lipid} . Unfortunately, determination of the exact mechanism leading to the observed variations associated with growth on pyruvate is not possible with the currently available information and further studies with isotopically labeled pyruvate could shed light on this issue.

4.2. Cultures grown at different temperatures and salinities

Cultures were grown at different temperatures and salt concentrations using media that contained yeast extract and peptone, both of which are mixtures of various compounds (e.g. carbohydrates, amino acids, proteins, etc.). These culture media can be expected to contain various carbohydrates and other compounds that can potentially be used as organic substrates. Therefore, only δD values of bulk yeast extract (-95‰) and peptone (-65‰) were measured. Therefore, these cultures are distinct from the cultures grown on defined substrates.

Previous studies with marine haptophytes (Schouten et al., 2006) and freshwater green algae (Zhang et al., 2009b) have shown that lipid δD values decrease with higher growth temperatures below the optimal growth temperature, and in the haptophyte *E. huxleyi*, lipid δD values increase again with further increase in temperature above the optimal growth temperature (Schouten et al., 2006; Zhang et al., 2009b). Changes in growth temperature affect organisms and their metabolism in multiple ways. For example, growth rates change with temperature (Schouten et al., 2006). Enzyme activities are also temperature dependent (Zhang et al., 2009b). In some cases, increasing temperature forces specific enzymes to be replaced by other higher temperature-tolerant enzymes (i.e. isoenzyme) that catalyze the same reaction (Zhang et al., 2009b). Organisms have also been observed to adopt different mechanisms of NADPH reduction (e.g. photosynthesis, pentose phosphate pathway), and other processes that affect the hydrogen isotope composition of NADPH such as hydrogen tunneling, in response to temperature change (Zhang et al., 2009b and references therein). All of these processes could be responsible for the observed influence of growth temperature on δD_{lipid} (Zhang et al., 2009b), which makes it difficult to decipher the specific influence of any one parameter. Moreover, temperature effects are also species dependent. For example, freshwater green algae show little change in growth rate with temperature change (Zhang et al., 2009b), whereas growth rates of marine haptophyte algae are substantially impacted along with their metabolic and

enzymatic activities (Schouten et al., 2006; Zhang et al., 2009b).

Our results for *H. marismortui* demonstrate that archaeol becomes more D-depleted (20.4‰) as temperature increases from 32 °C to 40 °C (Fig. 2a). This observation supports previous results, although the degree of D-depletion in our study is smaller compared to freshwater green algae (Zhang et al., 2009b) and marine haptophytes (Schouten et al., 2006). However, a reversal in the trend of D-depletion with increasingly higher temperature is observed above 40 °C with archaeol becoming D-enriched (11‰) at 45 °C compared to 40 °C (Fig. 2a). Growth rate of *H. marismortui* increases from 32 °C to 40 °C, and then slightly decreases again with further temperature increase to 45 °C, indicating that 40 °C is probably near the optimal growth temperature, which is also supported by previous studies (Camacho et al., 2009). This observation points towards changes in growth rate being the dominant factor resulting in the observed $\delta D_{\text{archaeol}}$ variations with temperature. Indeed, the pattern of archaeol D/H variation with temperature change in our experiments with *H. marismortui* is similar to the patterns measured for C_{37} and C_{38} alkenones from *Emiliania huxleyi* (Schouten et al., 2006), where alkenones became increasingly D-depleted as growth temperature was increased from 10 °C to 15 °C, and then became more D-enriched from 15 °C to 21 °C, 15 °C probably being the optimal growth temperature (Zhang et al., 2009b). However, it should also be mentioned that enzyme activities in *H. marismortui* do not mimic this pattern of growth rate with temperature, with esterase activity decreasing and lipase activity increasing with temperature increase (Camacho et al., 2009). Basic metabolic pathways (glycolysis, TCA cycle and the MVA biosynthetic pathway) involve many enzymes that can behave differently with temperature change and are thus not comparable. Due to a paucity of studies on *H. marismortui* enzyme responses with temperature and other growth conditions, it is difficult to ascertain whether (and to what extent) changes in enzyme activities also contribute to the observed temperature effect on $\delta D_{\text{archaeol}}$.

The impact of salt concentrations on D/H compositions of lipids have been studied from marine haptophyte algae in pure cultures (Schouten et al., 2006), cyanobacteria from Christmas Island saline ponds (Sachse and Sachs, 2008), and dinoflagellates from Chesapeake Bay (Sachs and Schwab, 2011). In all cases, higher salinity leads to D-enrichment of lipids. δD_{lipid} showed positive correlations with salinity, although different organisms are characterized with different slopes (Schouten et al., 2006; Sachse and Sachs, 2008; Sachs and Schwab, 2011). Sachs and Schwab (2011) attribute the observed D-enrichment to three possible mechanisms: (1) higher salinity reduces the exchange of water across the cell membrane. As a result, intracellular water will be recycled and become progressively D-enriched which will be subsequently reflected in lipids, (2) increased salinity leads to an increase in the synthesis of osmolytes (small organic compounds that help in balancing the external and internal salt concentrations), which would preferentially incorporate the H-isotope, leaving intracellular water more D-enriched, and (3) increasing salinity can cause a

decrease in growth rates resulting in reduced D/H fractionation between water and lipid and D-enrichment in lipids. It was also observed that the influence of salinity change on δD_{lipid} for halophilic cyanobacteria occurs during the metabolic processes that produce a precursor molecule, possibly pyruvate, and thus prior to the onset of lipid synthesis (Sachse and Sachs, 2008). Therefore, salinity change affects δD of pyruvate, which in turn is recorded by δD_{lipid} , but salinity change does not affect the lipid biosynthetic process itself (Sachse and Sachs, 2008).

Our results stand in contrast to previous observations. Archaeol synthesized by *H. marismortui* was more D-depleted (27‰) with increasing salinity from 23% to 25% (increasing NaCl concentration from 3.15 M to 3.4 M) with a reversal toward more D-enriched signatures (16‰) as salinity increased from 25% to 30% (NaCl concentration increasing from 3.4 M to 4.1 M; Fig. 2b; Table 3). Growth rates of *H. marismortui* increased with increasing salinity from 23% to 25% and decreased again with further salinity increase to 30%, indicating that 25% salinity is optimal for *H. marismortui* growth. Indeed, Optimal NaCl concentration for *H. marismortui* occurs from 3.4 to 3.9 M, and can grow in NaCl concentrations ranging from 1.7 to 5.1 M (Kletzin, 2007). Therefore, our results point towards changes in growth rate being the dominant factor resulting in the observed $\delta D_{\text{archaeol}}$ variations with salinity. However, the other mechanisms proposed by Sachs and Schwab (2011) should also be considered. If decreasing water exchange across the cell membrane was the dominant response to salinity change, we would expect archaeol to become consistently more D-enriched with increasing salt concentration, similar to the patterns observed in other studies (Schouten et al., 2006; Sachse and Sachs, 2008; Sachs and Schwab, 2011). However, this was not observed in our cultures. Further, production of osmolytes is not observed in halophilic archaea (Kletzin, 2007). Instead they have a different mechanism for adapting to high salinity that involves changes in amino acid compositions (Kletzin, 2007), that we believe will not significantly affect δD_{lipid} .

The pattern of $\delta D_{\text{archaeol}}$ variation is consistent for both temperature and salinity change and suggest an underlying mechanism that links salinity and temperature to D/H fractionation. Importantly, temperature and salinity both affect growth rate of *H. marismortui* in a similar way as observed in the current study and also supported by previous work (Camacho et al., 2009) and thus suggest that growth rate is the most important physiological factor impacting $\delta D_{\text{archaeol}}$ and D/H fractionation during lipid synthesis of *H. marismortui*. Higher growth rate is accompanied by greater D/H fractionation between water and lipids (Schouten et al., 2006; Zhang et al., 2009a; Sachs and Schwab, 2011). A probable mechanism by which growth rate affects δD_{lipid} is through H-isotope exchange between NADPH and water, which has been observed in vitro, resulting in a partial loss of D/H signal of NADPH, and can potentially occur in vivo (Zhang et al., 2009a). Previous experiments with heterotrophs provide evidence that isotope exchange between NADPH and water would be lower for faster growing organisms compared to slower growing organisms. Two heterotrophic bacteria studied by Zhang et al. (2009a)

grown on the same substrate produced lipids with markedly different δD , greater isotopic fractionation associated with faster growing organisms. Our results from *H. marismortui* cultures agree with this observation. However, isotope exchange between NADPH and water will depend on the steady-state turnover time of cellular NADPH, and due to a paucity of data on this turnover time, a definitive conclusion cannot be reached as to the exact mechanism by which growth rate affects δD_{lipid} .

4.3. Using archaeol as a proxy for δD_{water}

Archaeol δD values show good correlations with the δD of water in all cases, although the slopes and the intercepts vary depending on the substrate. Observed slopes of linear regressions of $\delta D_{\text{lipid}} - \delta D_{\text{water}}$ relationships are within the range reported from previous culture experiments (Zhang and Sachs, 2007; Zhang et al., 2009a). This indicates that archaeol can be potentially used as a proxy for water if arguments can be made that allow for the same organic substrate through time. However, in a natural environment different substrates can be available and variations in the proportions of available substrates (e.g. ratios of carbohydrates to TCA cycle intermediates) will cause $\delta D_{\text{archaeol}}$ to vary. Temperature and salinity also affect $\delta D_{\text{archaeol}}$, although on a smaller scale (20–30‰) compared to substrates (~100‰). Therefore, caution must be taken when using archaeol as a proxy for δD_{water} . Also, $\delta D_{\text{archaeol}} - \delta D_{\text{water}}$ relationships for other species of halophilic archaea should be thoroughly investigated to determine variability of this relationship among different species of halophilic archaea. Finally, further investigation is necessary in order to establish whether the isoprenoid chains released during diagenesis of archaeol, which can be preserved in sediments (Grice et al., 1998), will retain the primary δD compositions of the original archaeol molecule.

5. CONCLUSIONS

Our results indicate that the D/H composition of isoprenoid diether lipid archaeol synthesized by halophilic archaea correlates very well with the δD value of water in cultures. The organic substrate used during growth plays a critical role in determining the D/H fractionation during lipid synthesis by altering the metabolic pathways necessary to metabolize the specific substrate, and variations in the δD values of NADPH lead to the observed variations of $\delta D_{\text{archaeol}}$. Temperature and salinity also affect $\delta D_{\text{archaeol}}$ primarily by influencing *H. marismortui* growth rates. As a result, the most negative $\delta D_{\text{archaeol}}$ values occur at the optimal temperature and salinity conditions and subsequently increase under higher or lower temperatures and salinities. This correspondence strongly implicates the influence of growth rate on $\delta D_{\text{archaeol}}$. Changes in enzyme activities with temperature could also play a role on the expression of $\delta D_{\text{archaeol}}$ in addition to growth rate effects. However, the impact of different organic substrates on $\delta D_{\text{archaeol}}$ is approximately five times larger than the effects associated with temperature and salinity. Finally, while the δD value of archaeol is well correlated with the δD of

growth water, the impact of different organic substrates and growth conditions need to be carefully considered if archaeol is applied as a proxy for δD of ancient waters.

ACKNOWLEDGEMENTS

We would like to thank Dr. P.B. Moore at Yale University for providing us with the *H. marismortui* strain. We would also like to thank two anonymous reviewers, Dr. A.L. Sessions and Dr. R. Pancost for their comments that were helpful for the improvement of this manuscript.

APPENDIX A. SUPPLEMENTARY DATA

Supplementary data associated with this article can be found, in the online version, at <http://dx.doi.org/10.1016/j.gca.2013.05.023>.

REFERENCES

- Anderson I., Scheuner C., Göker M., Mavromatis K., Hooper S. D., Porat I., Klenk H.-P., Ivanova N. and Kyrpidis N. (2011) Novel insights into the diversity of catabolic metabolism from ten haloarchaeal genomes. *PLoS ONE* **6**, e20237. <http://dx.doi.org/10.1371/journal.pone.0020237>.
- Barker P. A., Street-Perrott F. A., Leng M. J., Greenwood P. B., Swain D. L., Perrott R. A., Telford R. J. and Ficken K. J. (2001) A 14,000-year oxygen isotope record from diatom silica in two alpine lakes on Mt. Kenya. *Science* **292**, 2307–2310.
- Boucher Y. (2007) Lipids: biosynthesis, function, and evolution. In *Archaea: Molecular Cell Biology* (ed. R. Cavicchioli). ASM Press, Washington, DC, pp. 341–353.
- Camacho R. M., Mateos J. C., González-Reynoso O., Prado L. A. and Córdova J. (2009) Production and characterization of esterase and lipase from *Haloarcula marismortui*. *J. Ind. Microbiol. Biotechnol.* **36**, 901–909.
- Chikaraishi Y., Suzuki Y. and Naraoka H. (2004) Hydrogen isotopic fractionations during desaturation and elongation associated with polyunsaturated fatty acid biosynthesis in marine macroalgae. *Phytochemistry* **65**, 2293–2300.
- Craig H. and Gordon L. I. (1965) Deuterium and oxygen 18 variations in the ocean and marine atmosphere. In *Stable Isotopes in Oceanographic Studies and Paleotemperatures* (ed. E. Tongiogi). Spoleto, Italy, pp. 9–130.
- Csonka L. N. and Fraenkel D. G. (1977) Pathways of NADPH formation in *Escherichia coli*. *J. Biol. Chem.* **252**, 3382–3391.
- Dansgaard W. (1964) Stable isotopes in precipitation. *Tellus* **16**, 436–468.
- Danson M. J., Lamble H. J. and Hough D. W. (2007) Central metabolism. In *Archaea: Molecular Cell Biology* (ed. R. Cavicchioli). ASM Press, Washington, DC, pp. 260–287.
- Dyall-Smith M. (2009) Media formulae and cultivation of haloarchaea. In *The Halohandbook, Version 7.2* (ed. M. Dyall-Smith). pp. 11–40.
- Falb M. (2005) Computational genome and pathway analysis of halophilic archaea. Dissertation, LMU München: Fakultät für Chemie und Pharmazie.
- Falb M., Müller K., Königsmaier L., Oberwinkler T., Horn P., von Gronau S., Gonzalez O., Pfeiffer F., Bornberg-Bauer E. and Oesterhelt D. (2008) Metabolism of halophilic archaea. *Extremophiles* **12**, 177–196.
- Gat J. R. (1996) Oxygen and hydrogen isotopes in the hydrologic cycle. *Annu. Rev. Earth Planet. Sci.* **24**, 225–262.
- Grice K., Schouten S., Nissenbaum A., Charrach J. and Sinnighe Damsté J. S. (1998) Isotopically heavy carbon in the C-21 to C-25 regular isoprenoids in halite-rich deposits from the Sdom Formation, Dead Sea Basin, Israel. *Org. Geochem.* **28**, 349–359.
- Hou J., Huang Y., Wang Y., Shuman B., Oswald W. W., Faison E. and Foster D. R. (2006) Postglacial climate reconstruction based on compound-specific D/H ratios of fatty acids from Blood Pond, New England. *Geochim. Geophys. Geosyst.* **7**, Q03008. <http://dx.doi.org/10.1029/2005GC001076>.
- Huang Y., Lockheart M. J., Collister J. W. and Eglinton G. (1995) Molecular and isotopic biogeochemistry of the Miocene Clarkia Formation: hydrocarbons and alcohols. *Org. Geochem.* **23**, 785–801.
- Huang Y., Shuman B., Wang Y. and Webb, III, T. (2002) Hydrogen isotope ratios of palmitic acid in lacustrine sediments record late Quaternary climate variations. *Geology* **30**, 1103–1106.
- Jouzel J., Lorius C., Petit J. R., Genthon C., Barkov N. I., Kotlyakov V. M. and Petrov V. M. (1987) Vostok ice core – a continuous isotope temperature record over the last climatic cycle (160,000 years). *Nature* **329**, 403–408.
- Kaneko M., Kitajima F. and Naraoka H. (2011) Stable hydrogen isotope measurement of archaeal ether-bound hydrocarbons. *Org. Geochem.* **42**, 166–172.
- Kletzin A. (2007) General characteristics and important model organisms. In *Archaea: Molecular Cell Biology* (ed. R. Cavicchioli). ASM Press, Washington, DC, pp. 14–92.
- Merlivat L. and Jouzel J. (1979) Global climatic interpretation of the deuterium–oxygen 18 relationship for precipitation. *J. Geophys. Res.* **84**, 5029–5033.
- Oren A., Ginzburg M., Ginzburg B. Z., Hochstein L. I. and Volcani B. E. (1990) *Haloarcula marismortui* (Volcani) sp. nov., nom. rev., an extremely halophilic bacterium from the Dead Sea. *Int. J. Syst. Bacteriol.* **40**, 209–210.
- Peteet D. M., Vogel J. S., Nelson D. E., Southon J. R., Nickmann R. J. and Heusser L. E. (1990) Younger dryas climatic reversal in northeastern USA? AMS ages for an old problem. *Quatern. Res.* **33**, 219–230.
- Qi H. and Coplen T. B. (2011) Investigation of preparation techniques for $\delta^2\text{H}$ analysis of keratin materials and a proposed analytical protocol. *Rapid Commun. Mass Spectrom.* **25**, 2209–2222.
- Sachs J. P. and Schwab V. F. (2011) Hydrogen isotopes in dinosterol from the Chesapeake Bay estuary. *Geochim. Cosmochim. Acta* **75**, 444–459.
- Sachse D., Radke J. and Gleixner G. (2004) Hydrogen isotope ratios of recent lacustrine sedimentary *n*-alkanes record modern climate variability. *Geochim. Cosmochim. Acta* **68**, 4877–4889.
- Sachse D. and Sachs J. P. (2008) Inverse relationship between D/H fractionation in cyanobacterial lipids and salinity in Christmas Island saline ponds. *Geochim. Cosmochim. Acta* **72**, 793–806.
- Sachse D., Kahmen A. and Gleixner G. (2009) Significant seasonal variation in the hydrogen isotopic composition of leaf-wax lipids for two deciduous tree ecosystems (*Fagus sylvatica* and *Acer pseudoplatanus*). *Org. Geochem.* **40**, 732–742.
- Sauer P. E., Eglinton T. I., Hayes J. M., Schimmelmann A. and Sessions A. L. (2001) Compound-specific D/H ratios of lipid biomarkers from sediments as a proxy for environmental and climatic conditions. *Geochim. Cosmochim. Acta* **65**, 213–222.
- Savin S. M. and Epstein S. (1970) The oxygen and hydrogen isotope geochemistry of clay minerals. *Geochim. Cosmochim. Acta* **34**, 25–42.
- Schefeß E., Schouten S. and Schneider R. R. (2005) Climatic controls on central African hydrology during the past 20,000 years. *Nature* **437**, 1003–1006.

- Schouten S., Ossebaar J., Schreiber K., Kienhuis M. V. M., Langer G., Benthien A. and Bijma J. (2006) The effect of temperature, salinity and growth rate on the stable hydrogen isotopic composition of long chain alkenones produced by *Emiliania huxleyi* and *Gephyrocapsa oceanica*. *Biogeosciences* **3**, 113–119.
- Sessions A. L., Burgoyne T. W., Schimmelmann A. and Hayes J. M. (1999) Fractionation of hydrogen isotopes in lipid biosynthesis. *Org. Geochem.* **30**, 1193–1200.
- Sessions A. L., Jahnke L. L., Schimmelmann A. and Hayes J. M. (2002) Hydrogen isotope fractionation in lipids of the methane-oxidizing bacterium *Methylococcus capsulatus*. *Geochim. Cosmochim. Acta* **66**, 3955–3969.
- Shuman B., Webb, III, T., Bartlein P. and Williams J. W. (2002) The anatomy of a climatic oscillation: vegetation change in eastern North America during the Younger Dryas chronozone. *Quatern. Sci. Rev.* **21**, 1777–1791.
- Shuman B., Huang Y., Newby P. and Wang Y. (2006) Compound-specific isotopic analyses track changes in seasonal precipitation regimes in the Northeastern United States at ca 8200 cal yr BP. *Quatern. Sci. Rev.* **25**, 2992–3002.
- Smith F. A. and Freeman K. H. (2006) Influence of physiology and climate on δD of leaf wax *n*-alkanes from C₃ and C₄ grasses. *Geochim. Cosmochim. Acta* **70**, 1172–1187.
- Stern L. A., Chamberlain C. P., Reynolds R. C. and Johnson G. D. (1997) Oxygen isotope evidence of climate change from pedogenic clay minerals in the Himalayan molasse. *Geochim. Cosmochim. Acta* **61**, 731–744.
- Stiehl T., Rullkötter J. and Nissenbaum A. (2005) Molecular and isotopic characterization of lipids in cultured halophilic microorganisms from the Dead Sea and comparison with the sediment record of this hypersaline lake. *Org. Geochem.* **36**, 1242–1251.
- Xie S., Nott C. J., Avsejs L. A., Volders F., Maddy D., Chambers F. M., Gledhill A., Carter J. F. and Evershed R. P. (2000) Palaeoclimate records in compound-specific δD values of a lipid biomarker in ombrotrophic peat. *Org. Geochem.* **31**, 1053–1057.
- Yamanaka T., Shimada J., Hamada Y., Tanaka T., Yang Y., Zhang W. and Hu C. (2004) Hydrogen and oxygen isotopes in precipitation in the northern part of the North China Plain: climatology and inter-storm variability. *Hydrol. Process.* **18**, 2211–2222.
- Yang H. and Huang Y. (2003) Preservation of lipid hydrogen isotope ratios in Miocene lacustrine sediments and plant fossils at Clarkia, northern Idaho, USA. *Org. Geochem.* **34**, 413–423.
- Zhang X., Gillespie A. L. and Sessions A. L. (2009a) Large D/H variations in bacterial lipids reflect central metabolic pathways. *Proc. Nat. Acad. Sci. U.S.A.* **106**, 12580–12586.
- Zhang Z. and Sachs J. P. (2007) Hydrogen isotope fractionation in freshwater algae: I. Variations among lipids and species. *Org. Geochem.* **38**, 582–608.
- Zhang Z., Sachs J. P. and Marchetti A. (2009b) Hydrogen isotope fractionation in freshwater and marine algae: II. Temperature and nitrogen limited growth rate effects. *Org. Geochem.* **40**, 428–439.

Associate editor: Richard Pancost